

Environmental effects on the maturation of the endodermis and multiseriate exodermis of *Iris germanica* roots

Chris J. Meyer¹, James L. Seago Jr² and Carol A. Peterson^{1*}

¹Department of Biology, University of Waterloo, 200 University Avenue W, Waterloo, Ontario, N2L 3G1, Canada and

²Department of Biological Sciences, State University of New York, Oswego, NY 13126, USA

Received: 29 September 2008 Returned for revision: 28 October 2008 Accepted: 17 November 2008 Published electronically: 16 January 2009

- **Background and Aims** Most studies of exodermal structure and function have involved species with a uniseriate exodermis. To extend this work, the development and apoplastic permeability of *Iris germanica* roots with a multiseriate exodermis (MEX) were investigated. The effects of different growth conditions on MEX maturation were also tested. In addition, the exodermises of eight *Iris* species were observed to determine if their mature anatomy correlated with habitat.
- **Methods** Plants were grown in soil, hydroponics (with and without a humid air gap) or aeroponics. Roots were sectioned and stained with various dyes to detect MEX development from the root apical meristem, Casparian bands, suberin lamellae and tertiary wall thickenings. Apoplastic permeability was tested using dye (berberine) and ionic (ferric) tracers.
- **Key Results** The root apical meristem was open and MEX development non-uniform. In soil-grown roots, the exodermis started maturing (i.e. Casparian bands and suberin lamellae were deposited) 10 mm from the tip, and two layers had matured by 70 mm. In both hydro- and aeroponically grown roots, exodermal maturation was delayed. However, in areas of roots exposed to an air gap in the hydroponic system, MEX maturation was accelerated. In contrast, maturation of the endodermis was not influenced by the growth conditions. The mature MEX had an atypical Casparian band that was continuous around the root circumference. The MEX prevented the influx and efflux of berberine, but had variable resistance to ferric ions due to their toxic effects. *Iris* species living in well-drained soils developed a MEX, but species in water-saturated substrates had a uniseriate exodermis and aerenchyma.
- **Conclusions** MEX maturation was influenced by the roots' growth medium. The MEX matures very close to the root tip in soil, but much further from the tip in hydro- and aeroponic culture. The air gap accelerated maturation of the second exodermal layer. In *Iris*, the type of exodermis was correlated with natural habitat suggesting that a MEX may be advantageous for drought tolerance.

Key words: *Iris germanica*, roots, culture conditions, development, anatomy, apoplastic tracers, multiseriate exodermis, endodermis, root apical meristem.

INTRODUCTION

An exodermis is present in the majority of angiosperm roots tested (Perumalla *et al.*, 1990; Peterson and Perumalla, 1990) and an endodermis is present in all roots so far tested except for some members of the Lycopodiaceae (see Clarkson, 1996; Damus *et al.*, 1997; D. E. Enstone, University of Waterloo, Canada, pers. comm.). The development of the highly specialized cells of these two layers progresses through as many as three states as described by Van Fleet (1961), Esau (1965) and Robards *et al.* (1973). In roots of most species, the endodermis starts to mature before the exodermis, but the sequence of development is roughly the same in cells of both layers. The first developmental state (State I) is reached when Casparian bands are formed in the anticlinal walls. At this time, there is a tight connection between the modified wall and the adjacent plasmalemmas of the cells (Bonnett, 1968; Enstone and Peterson, 1997; Karahara and Shibaoka, 1992; Ma and Peterson, 2001). Isolated Casparian bands are composed predominantly of lignin phenolics, along with aliphatic suberin, cell wall

carbohydrates and proteins (Zeier and Schreiber, 1998). Next, during the second developmental state (State II), a suberin lamella is deposited around the protoplast (i.e. between plasmalemma and wall). This lamella severs the connection between the Casparian band and plasmalemma (Robards *et al.*, 1973; Haas and Carothers, 1975; Ma and Peterson, 2001). According to Kolattukudy (1980), Zeier and Schreiber (1998) and Bernards (2002), suberin lamellae consist mainly of poly(aliphatic) and poly(phenolic) suberin monomers, as well as glycerol and associated waxes; cell wall proteins and polysaccharides were also detected in their isolates of the lamellae. Lastly, in the third developmental state (State III), tertiary cellulosic walls that are often lignified (Zeier and Schreiber, 1998) are laid down along the suberin lamellae. These depositions can be U-shaped and thick enough to mask the identification of Casparian bands and suberin lamellae (Van Fleet, 1961; Esau, 1965; Clarkson *et al.*, 1987). In the endodermis, there is typically a gap between the development of the Casparian bands, suberin lamellae and tertiary walls, whereas in the exodermis the situation is more variable. In the uniform exodermis, the Casparian bands and suberin lamellae are normally deposited

* For correspondence. E-mail cpeterson@uwaterloo.ca

simultaneously. But in the dimorphic exodermis, development of suberin lamellae and tertiary walls is delayed in the short cells (von Guttenberg, 1968; Peterson and Enstone, 1996; Enstone and Peterson, 1997). The rate at which individual cells mature within the exodermis and endodermis can vary; it is common to observe some cells of the dimorphic exodermis and endodermis in older parts of roots that have only matured to State I. These cells have Casparian bands but lack suberin lamellae and tertiary walls, and are called passage cells (Esau, 1965; von Guttenberg, 1968). In the uniform exodermis, concurrent deposition of Casparian bands and suberin lamellae can be patchy or variable along the root. Since immature cells in the uniform exodermis lack Casparian bands, they are not referred to as passage cells (Enstone and Peterson, 1997). In a broader context, this variation in maturation rates, in addition to other modifications, can allow a plant species to become specialized in order to exploit specific environmental conditions.

The exodermis is known to vary in structure among species (Kroemer, 1903; Perumalla *et al.*, 1990; Peterson and Perumalla, 1990; Hose *et al.*, 2001). To date, most root structure and function research has focused on species with a single-layered (uniseriate) exodermis, including *Zea mays*, *Oryza sativa* and *Allium cepa* (Perumalla *et al.*, 1990; Miyamoto *et al.*, 2001; see Enstone *et al.*, 2003 and references therein; Ranathunge *et al.* 2003, 2004, 2005a, b). A less common type of exodermis that has received little attention is the multi-layered or multiseriate exodermis (MEX) such as that found in *Iris germanica* (Kroemer, 1903; Shishkoff, 1986; Peterson and Perumalla, 1990; Zeier and Schreiber, 1998), *Typha* spp. (Seago and Marsh, 1989; Seago *et al.*, 1999) and *Phragmites australis* (Armstrong *et al.*, 2000; Soukup *et al.*, 2002). The exodermal Casparian band in these species is atypical because, instead of being confined to the anticlinal walls, it also extends into the tangential walls of the adjacent layers of the exodermis. Since this Casparian band deposition follows the exodermal wall continuum, the band often appears H- or Y-shaped in cross-section. Roots of *I. germanica*, in particular, are of interest as they have been the subject of some basic anatomical studies (Kroemer, 1903; Shishkoff, 1986; Peterson and Perumalla, 1990) and biochemical work (Zeier and Schreiber, 1998, 1999). In these articles, brief descriptions of exodermal ontogeny and structure were provided, but a thorough investigation that combined the development of all root tissues was lacking. Furthermore, the distribution of *Iris* is global with many species inhabiting diverse natural habitats such as wetlands and well-drained soils, allowing observation of potential correlations between root anatomy and habitat.

The timing and rates at which exodermal and endodermal tissues mature depend on environmental cues and how these cues influence the regulation of expression of developmental genes (see Bray *et al.*, 2000; Enstone *et al.*, 2003). Plant species that are native to particular ecosystems have evolved constitutive resistances to local environmental stresses. However, if these stresses increase in severity or duration, or if a new stress is encountered, the species must acclimate or otherwise risk death (Bray *et al.*, 2000). Acclimation occurs, in part, by regulation of the onset and rapidity of tissue development or its modification. In roots the exodermis, for

example, is known to respond to changes in the substrate (see Enstone *et al.*, 2003). Like Clarkson *et al.* (1987), Enstone and Peterson (1998) exposed basal parts of *Z. mays* roots to humid air inside hydroponic chambers. After 2 d, 92 % of the exodermal cells in the exposed part of the root were in State II compared with 11 % of the cells of the same age in submerged roots. Exodermal suberin lamellae formation was also accelerated in *Z. mays* grown in aeroponics, vermiculite or in a stagnant (oxygen-deficient) solution compared with aerated hydroponics (Zimmermann and Steudle, 1998; Enstone and Peterson, 2005). In contrast, the developmental reactions of a MEX to various growth conditions have not been investigated.

The present paper provides details of the origin and maturation of *I. germanica*'s exodermis and endodermis, layers flanking the parenchymatous central cortex. The effects of varying growth conditions on maturation of these layers were explored. Additionally, the apoplastic permeability of its MEX was tested using dye (berberine) and ionic (ferric) tracers. To establish a suitable treatment time and concentration for the latter, a toxicity test using *Zea mays* seedlings with rapid root growth was performed. *Iris germanica* roots were amenable to permeability tests because they generated very few lateral roots, leaving the exodermis intact, a trait not shared by *Typha* and *Phragmites*. Lastly, the mature root anatomy of seven other iris species was compared with that of *I. germanica* to determine if the root anatomy among species of this genus is correlated with their natural habitats.

MATERIALS AND METHODS

Plant material and growth conditions

Vegetative plants (rhizomes, with their leaves and subtending roots) of 25 *Iris germanica* L. cultivars (Table S1 in Supplementary material, available online) and five additional species [*I. pumila* L. (origin), *I. pallida* Lam. ('Argenteo Variegata'), *I. sibirica* L. ('Super Ego' and 'Violet Flare'), *I. spuria* L. ('Amber Ripples' and 'White Olinda') and *I. versicolor* L. ('Blue Flag')] were collected from outdoor plots at the Royal Botanical Gardens in Burlington, Ontario in early August 2005. They were transplanted in potting soil (Pro-Mix, Premier Horticulture Inc., Dorval, Quebec) and placed in a growth chamber (light 300 $\mu\text{mol m}^{-2} \text{s}^{-1}$ PAR, 16-h day, 25 °C day, 23 °C night, RH 65 %). To obtain roots for testing, the rhizomes and attached roots were carefully lifted from the soil after 30–45 d. Then healthy looking adventitious roots, between 150–200 mm in length, were excised from the rhizome under water with a razor blade and rinsed to remove most of the soil. Roots used for anatomical analysis were stored in 70 % ethanol and kept in a refrigerator (4 °C). Roots that were tested for apoplastic permeability were used immediately after excision from the rhizome. Roots from two additional species, *I. hexagona* and *I. pseudacorus*, were preserved in 70 % ethanol and kept for anatomical observation (courtesy of S. Mopper, University of Louisiana, Lafayette, USA).

Iris germanica plants were also collected from outdoor plots at the University of Bayreuth, Germany, in May 2006, transplanted into potting soil, and placed in a growth chamber.

After 30–45 d, some were gently unearthed and transferred to hydroponic or aeroponic culture. The nutrient solution was 0.09 mM $(\text{NH}_4)_2\text{SO}_4$, 0.07 mM MgSO_4 , 0.06 mM $\text{Ca}(\text{NO}_3)_2$, 0.05 mM KH_2PO_4 , 0.05 mM KNO_3 , 0.05 mM Fe(III)-EDTA, 0.03 mM K_2SO_4 , 4.6 μM H_3BO_3 , 1.8 μM MnSO_4 , 0.3 μM ZnSO_4 , 0.3 μM CuSO_4 ; pH 5.5–6.0. All the hydroponic tanks were completely filled with solution until new roots, produced subsequent to transfer, were longer than 65 mm. Some tanks remained full of nutrient solution (control, Fig. 1A) while others were only partially filled during the weekly nutrient exchange to create an air gap of approx. 60 mm between the base of the rhizome and solution surface (Fig. 1B). These rhizomes were wrapped in paper towel saturated with nutrient solution to prevent them from drying. The humidity in the air gap was measured with a digital hygrometer/thermometer (Control Company; Friendswood, TX, USA). The nutrient solution was constantly aerated using a single bubbling stone and was replaced with fresh solution weekly. The aeroponic chamber was a cylinder (1 m diameter, 1 m high) that could hold two rhizomes. A humidifier ('Defensor'; Barth and Stöcklein, Garching, Germany) that continuously produced a mist of nutrient solution was placed in this chamber (Fig. 1C). A high humidity was thus obtained, and nutrient solution was observed dripping from the roots.

Root anatomy

To observe *I. germanica*'s root apical meristem and origin of the MEX, 4–10 mm long roots were used. After excising these roots from the rhizome, they were vacuum infiltrated

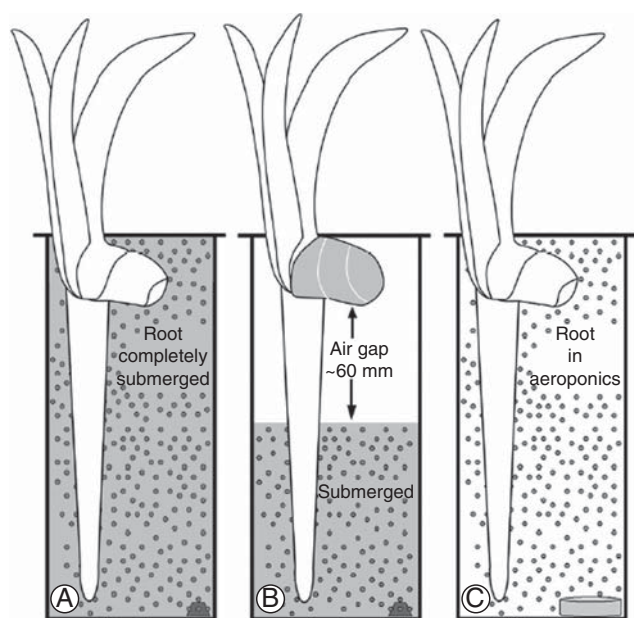


FIG. 1. Drawings of the hydroponic (A), air gap (B) and aeroponic (C) systems used to expose iris roots to various conditions (not to scale). (A) Roots and rhizomes were completely submerged in hydroponic nutrient solution. (B) A partially filled hydroponic tank with an air gap between the base of the root (attached to the rhizome) and the surface of the solution. Nutrient solutions were constantly aerated with atmospheric air using bubbling stones (trapezoids). (C) Roots and rhizomes were completely saturated from continuous misting with a humidifier (grey cylinder) in an aeroponic tank.

with 4% formaldehyde in glacial acetic acid (FAA), left submerged in FAA for 2–3 d, then rinsed and stored in 70% ethanol. The fixed root specimens were embedded in Paraplast Plus (Sherwood Medical Industries; DeLand, FL, USA) and cross-sectioned with a microtome at 8–10 μm increments from the root tip. Median longitudinal sections were also taken. Sections were stained with safranin/fast green and viewed with white light (Seago and Marsh, 1989).

Root structure, especially key exodermal and endodermal developmental stages, was observed in detail along the length (all areas from the tip to 20 mm, and then at intervals of 10 mm up to 150–200 mm) of at least ten roots for *I. germanica*, grown in the different conditions described above. Additionally, the anatomy 150–200 mm from the tip was observed for at least three roots from each of the 25 *I. germanica* cultivars. For all other species, the anatomy of at least five roots each was observed at 90–120 mm from the tip. Roots were freehand sectioned transversely or longitudinally at various distances from the root tip and then subjected to several staining procedures. These were Sudan red 7B and Fluorol yellow 088 for lipids including suberin lamellae (Brundrett *et al.*, 1991), berberine hemisulfate–aniline blue for Casparian bands (Brundrett *et al.*, 1988), phloroglucinol–HCl for lignin (Jensen, 1962) and TBO as a general polychromatic stain (O'Brien *et al.*, 1964).

The removal or clearing of cellular protoplasts can be advantageous when studying cell wall structure. Recently, Lux *et al.* (2005) reported new approaches for simultaneously clearing and staining tissue. Basically, the fluorochromes 0.1% berberine hemisulfate and 0.01% Fluorol yellow were dissolved in a clearing mixture consisting of pure lactic acid saturated with chloral hydrate. In the present study, iris root sections were incubated in either of the two dye solutions at 70 °C for 1 h. In the case of berberine hemisulfate, sections were counterstained with 0.5% aniline blue (dissolved in dH_2O) at room temperature for 30 min. All specimens were viewed with ultraviolet (UV) light. In addition to the clearing, physical separation of the central region (endodermis and stele) from the rest of the root tissue was possible. To achieve this, root segments were cut longitudinally with a razor blade through the central cortex, and then the loosely adhering epidermal, exodermal and central cortical tissues were peeled off using fine-tipped forceps. This allowed a clear longitudinal view of the endodermal cells so that their passage cells and cell lengths could be observed.

Results of all staining procedures were compared with control, unstained sections. These were viewed with either white or UV light as appropriate.

Sulfuric acid digestion was also used which reportedly spares suberized and cutinized tissue (Johansen, 1940). Sections of roots were bathed in a drop of concentrated sulfuric acid on a slide for 24 h at room temperature.

Specimens were examined with Zeiss epifluorescence microscopes with either white or UV light (filter set: exciter filter G 365, dichroitic mirror FT 395, and barrier filter LP 420; Carl Zeiss, Inc.). Photographs were taken with a Q-Imaging digital camera (Retiga 2000R, Fast 1394, Cooled Mono, 12-bit; Quorum Technologies Inc., Guelph, ON) or a Cool Snap digital camera (Visitron Systems, Puchheim, Germany).

Iris germanica root growth rate measurements

Growth rates were estimated for soil-grown roots ($n = 9$) and hydroponically grown roots that were completely submerged ($n = 10$) or exposed to the air gap ($n = 10$). An initial measurement of root length was made (length = 40–70 mm), and 5 or 6 d later a second measurement was taken. Root tips did not contact the sides or bottoms of either the pots or hydroponic chambers during the growth measurement period. Data were analysed with a one-way analysis of variance (ANOVA) at $P \leq 0.05$ (Statistix Student Ed., v. 2.0). The ages of root regions where key maturation processes occurred were calculated by assuming the roots grew uniformly during the period of measurement.

Apoplastic permeability

Soil-grown *I. germanica* roots were excised from the rhizome under water and then cut into 30–40 mm long segments. The cut ends were blotted dry with tissue paper and then sealed with molten sticky wax (Kerr Manufacturing Canada, Mississauga, ON) prior to treatment. Two apoplastic tracers were employed to test the permeability of the exodermis. At least five roots were used for each tracer test. Several controls were run: (1) unstained sections (to observe native pigmentation or autofluorescence); (2) sections stained with the tracers (to confirm that cells exposed to the tracers would be stained); and (3) peripheral layers (i.e. epidermis, exodermis and part of the central cortex) severed by a longitudinal cut prior to tracer application (to test the permeability of the central cortex).

Berberine hemisulfate. As described by Enstone and Peterson (1992) excised, sealed roots were bathed in 0.05 % berberine hemisulfate for 1 h followed by 0.05 M potassium thiocyanate for 1 h. In some cases, a short, longitudinal incision was made with a razor blade through the peripheral layers so that the dye could bypass the exodermis and enter the central cortex. This allowed for exodermal permeability from the inside to be tested. Roots were freehand-sectioned and viewed with UV light as described above.

Ferrous sulfate toxicity test. Thirty germinated kernels of *Zea mays* L. ('Seneca Horizon'; Ontario Seed Co., Waterloo, ON) with root lengths of 30–40 mm and emerged coleoptiles were transferred to aerated hydroponic culture in a glasshouse under ambient lighting. The culture solution consisted of 0.7 mM K_2SO_4 , 0.5 mM $Ca(NO_3)_2$, 0.5 mM $MgSO_4$, 0.1 mM KCl, 0.1 mM KH_2PO_4 , 0.01 mM Fe(III)-EDTA, 1.0 μM H_3BO_3 , 0.5 μM $MnSO_4$, 0.5 μM $ZnSO_4$ and 0.2 μM $CuSO_4$. The hydroponic system (with light-proof walls) was assembled as previously described (Enstone and Peterson, 1998). Kernels were placed on a floating styrofoam sheet with holes to accommodate the roots. This was then covered with two sheets of cheesecloth that hung into the solution to keep the kernels hydrated. The top of each hydroponic tank was covered with two layers of shading cloth to reduce light transfer from above into the tank. After 2 d in the hydroponic solution, the root lengths of all seedlings were measured. The roots were then exposed to ferrous sulfate ($FeSO_4 \cdot 7H_2O$) at different concentrations. Six large, glass test tubes (60 mL) were jacketed

with aluminium foil and completely filled with a desired concentration of $FeSO_4$ (0.25 mM in one tube, 0.5 mM in three tubes, and 1.0 mM in one tube) or with nutrient solution (one tube). The top of each tube was covered with flexible, laboratory film (Parafilm) in which small slits had been made to allow the roots to enter the solution while supporting the kernels above. Five seedlings were placed in each tube. Roots were exposed to the nutrient solution, 0.25 and 1 mM $FeSO_4$ treatments for 2 h; the duration of the 0.5 mM $FeSO_4$ treatment was 1, 2 or 3 h (hence the need for three tubes containing this concentration). Following the intended exposure time, the seedlings were transferred back to the original hydroponic tank and grown for 3 more days during which the root lengths were measured daily. This toxicity experiment was conducted twice. Growth rate data were analysed using a one-way ANOVA with a least significant differences (LSD) *post hoc* test at $P \leq 0.05$ (Statistix Student Ed., v. 2.0).

Ferrous sulfate permeability. This method was modified from de Rufz de Lavison (1910), Soukup *et al.* (2002) and Armstrong and Armstrong (2005), considering the results from the toxicity test above. *Iris germanica* roots were incubated in 0.5 mM $FeSO_4$ for 1 h. To test exodermal permeability from the inside, the peripheral layers of some roots were cut open as described above, allowing the $FeSO_4$ to enter the central cortex. After treatment, all roots were rinsed with running water for 30 min and then sectioned freehand. The sections were placed in a drop of 1 mM potassium ferrocyanide ($K_4[Fe(CN)_6] \cdot 3H_2O$) dissolved in 0.5 % HCl on a slide for 2–3 min. During this time, a 'Prussian blue' precipitate of ferric ferrocyanide ($Fe_4[Fe(CN)_6]_3$) formed in the areas where the ferric ions had entered (Pearse, 1968). [According to Guerinet and Yi (1994), in the eudicots and non-graminaceous monocots (such as *I. germanica*), ferric ions are restricted to the apoplast while ferrous ions can be transported across the plasmalemma.] Sections were observed using the microscope described above (with white light).

The potential toxicity of $FeSO_4$ and its effect on the apoplastic permeability of *I. germanica* roots were tested. Sealed root segments were incubated in 0.5 mM $FeSO_4$ or water (i.e. control) for 1 h, followed by rinsing with running water for 30 min. These root segments were then submerged in 0.05 % berberine hemisulfate for 1 h, rinsed with water, cross-sectioned, and viewed with UV light.

RESULTS

Iris germanica root growth and anatomy

Root growth rates (mean \pm s.d.) for soil-grown roots (14.7 ± 1.9 mm d^{-1}), submerged hydroponically grown roots (14.7 ± 2.3 mm d^{-1}) and air gap roots (14.8 ± 1.9 mm d^{-1}) were the same statistically (ANOVA; $P = 0.99$). With these data, it was possible to relate the age of specific root regions to their distances from the tip.

Root anatomy was virtually identical among the 25 cultivars of *Iris germanica* observed (listed in Table S1 in Supplementary material, available online). The following data are from the cultivar 'Paradise'. Unless otherwise noted, data are from primary, adventitious roots originating in the rhizome.

Root apical meristem. Close examination of *I. germanica*'s root apical meristem revealed that it was an open type with multiple files of cortex cell precursors (Fig. 2A–C). There was no temporal regularity of increase in the number of immature exodermal cell files. After differentiation from the exodermal initial, subsequent immature exodermal cell divisions were

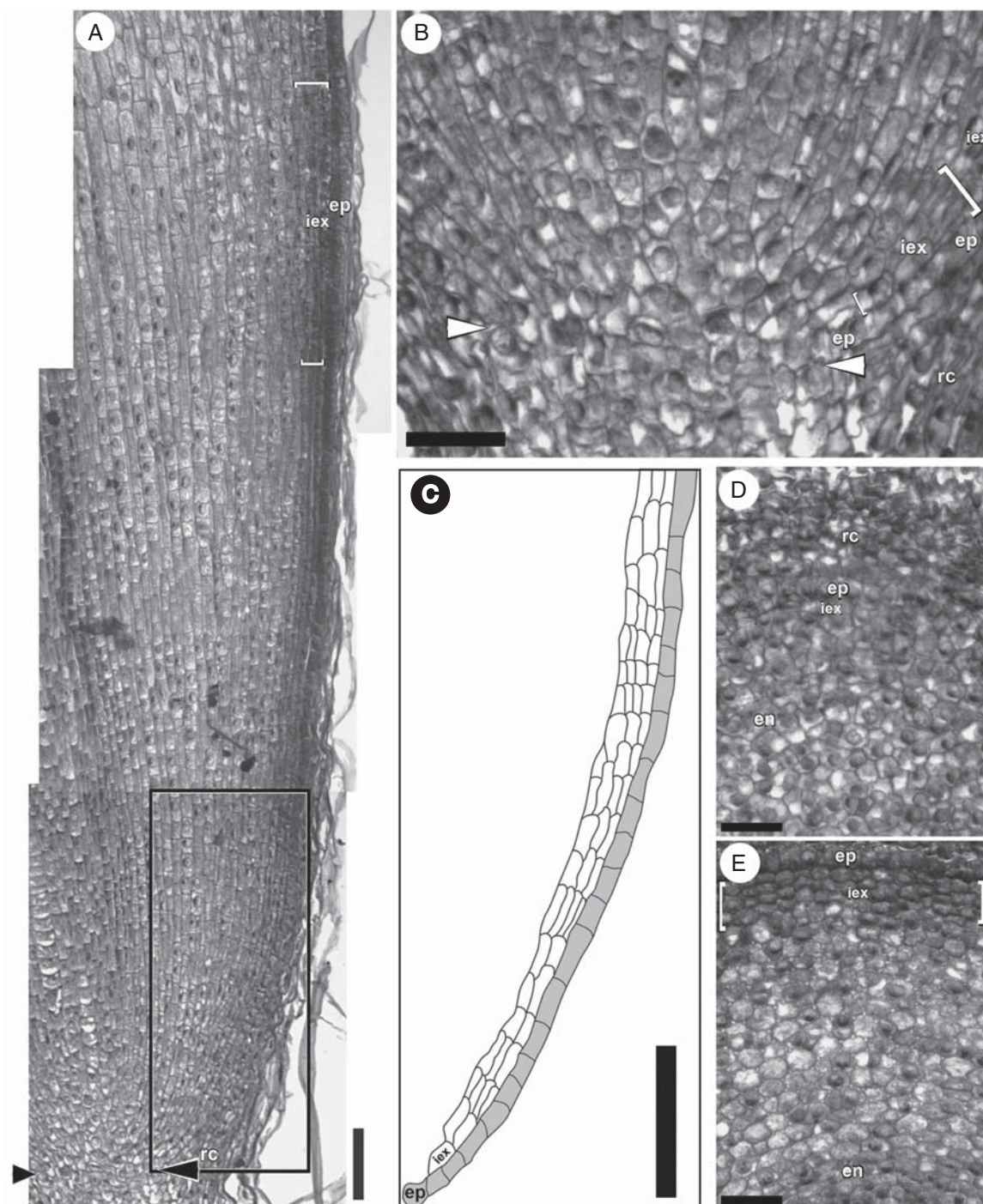


FIG. 2. *Iris germanica* adventitious root tips in (A, B) longitudinal and (D, E) transverse sections. (A) Tip of a 4-mm-long adventitious root. Arrowheads indicate the distal extremity of the root apical meristem. (B) Enlargement of the apical meristem area (arrowheads as in A). The epidermis is immature and the number of developing immature exodermal cell files varies (within square brackets). (C) Tracing of the immature epidermal (grey) and exodermal (white) cells, located in the rectangle outlined in (A). Note the variable number of immature exodermal cell files in this region. (D) Section 50 μm from the tip of the root proper. Note the lack of regular radial alignments of cells across the young cortex. The root cap is thick at this distance. (E) Section 200 μm from the tip of the root proper. A boundary between the epidermis and immature exodermis is noticeable at this distance. There are two to four layers of cells in the immature exodermis, which are characterized by a lack of intercellular air spaces (within square brackets). Abbreviations: Rc, root cap; ep, epidermis; iex, immature exodermis; en, endodermis. Scale bars: (A, C) = 100 μm ; (B, D, E) = 50 μm .

irregular over time, forming files ranging from two to four near the root tip (Fig. 2A, C). Furthermore, there were no apparent radial cell alignments across the central cortex, i.e. between the immature exodermis and the endodermis (Fig. 2D, E); this was related to the open nature of the root apical meristem as well as to the non-uniform anticlinal and periclinal cell divisions within it.

Soil-grown roots: outer layers. In the outermost layer of the exodermis, Casparian bands in the anticlinal walls and suberin lamellae formed concurrently and were first detected 10–15 mm from the root tip (Fig. 3A, B). Initially, Casparian bands appeared in two separate locations in each anticlinal and transverse wall, but they rapidly extended through these walls to form one continuous band. By 20 mm from the root tip, most of the exodermal cells contained typical Casparian bands and suberin lamellae. At 30 mm from the tip, a second exodermal layer started to differentiate centripetal to the first layer. The first indication of this was the extension of the Casparian band into the inner tangential walls of the first layer and the outer tangential walls of the second layer. As the root aged, the band extended into the anticlinal walls

of the second layer. While the second exodermal layer continued to mature, very thin lignified tertiary walls formed in the first layer. It was not until 70 mm from the tip that the second exodermal layer had completed its maturation (Fig. 3C, D). At this bi-layered stage, the extension of the Casparian bands through adjoining tangential walls created a continuous circumferential Casparian band (ccCb). Depending on the arrangement of the exodermal cells, this Casparian band was either Y- or H-shaped when viewed in cross-section (Fig. 3C). Maturation of the third exodermal layer was complete at 100 mm from the tip with continued extension of the Casparian band through the tangential and anticlinal walls of the adjacent cells (Fig. 3E), as well as suberin lamella deposition (Fig. 3F, G) and lignification of the thin tertiary walls (Fig. 3H) of this third cell layer. Proximal to this area, an ultimate fourth exodermal layer could mature in the sequence described above. When the tissue was digested with sulfuric acid, all walls of the mature exodermis were retained (data not shown). To observe cell lengths, it was necessary to use longitudinal views because, in transverse view, long and short cells would be indistinguishable. In the MEX, an irregular dimorphism was observed in the

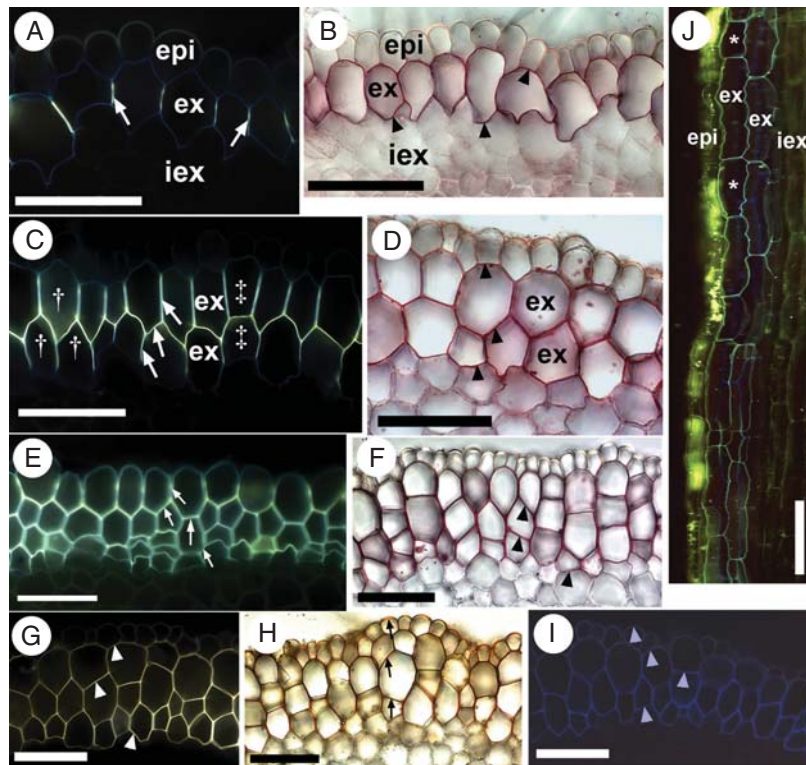


FIG. 3. Photomicrographs of the outer part of *I. germanica* roots in (A–I) cross- and (J) longitudinal section. Values in millimetres refer to distances from the root tips. (A) 15 mm. Stained with berberine hemisulfate–aniline blue. Casparian bands (white arrows) fluoresced yellow and occupied the anticlinal walls of the outermost exodermal layer. (B) 15 mm. Stained with Sudan red 7B. Suberin lamellae (black arrowheads) appeared as red rings in the walls of the outermost exodermal layer. (C) 70 mm. Stained with berberine hemisulfate–aniline blue. The ccCb (white arrows) was Y-shaped (in cells labelled with †) or H-shaped (in cells labelled with ‡). (D) 70 mm. Stained with Sudan red 7B. Cells in the two mature exodermal layers contained suberin lamellae (black arrowheads). (E) 100 mm. Stained with berberine hemisulfate–aniline blue. The ccCb (white arrows) filled the anticlinal and tangential walls of cells in the multiserial exodermis. (F) 100 mm. Stained with Sudan red 7B. Cells in the multiserial exodermis all contained suberin lamellae (black arrowheads). (G) 100 mm. Stained with Fluorol yellow 088. Suberin (white arrowheads) fluoresced yellow in exodermal cell walls. (H) 100 mm. Stained with phloroglucinol–HCl. Lignin (black arrows) appeared reddish-orange in the walls of epidermal and exodermal cells. (I) 70 mm. Autofluorescence with UV light. Walls of the epidermis and exodermis autofluoresced faint blue (light blue arrowheads). (J) 70 mm. Epidermal cells containing berberine thiocyanate crystals (yellow) and a dimorphic, biserial exodermis with blue, autofluorescent walls. Asterisks indicate short cells. Abbreviations: epi, epidermis; ex, mature exodermis; iex, immature exodermis. Scale bars = 100 μ m.

first layer (i.e. short cells were present but did not regularly alternate with long cells), but not in the underlying layers (Fig. 3J). The shorter cells differed from the longer cells only in length; all cells had Casparian bands, suberin lamellae and thin tertiary wall thickenings.

In the epidermis, the cells were tabular and uniform (data not shown). Their walls did not stain for lipids (Fig. 3G) but did stain positively for lignin (Fig. 3H) in addition to being faintly autofluorescent under UV light (Fig. 3I) at all distances from the root tip that were investigated. All epidermal walls were digested by sulfuric acid (not shown).

Soil-grown roots: inner parts. In the endodermis, the initial Casparian bands formed 10–15 mm from the root tip (i.e. the same distance as did the exodermis). These bands appeared as small dots in cross-section and were located very close to the pericycle. Also at this distance, lignin was detected in the outer tangential walls of all the endodermal cells and in the walls of protoxylem vessels. Suberin lamellae were

first detected in the endodermis 20 mm from the root tip. At 30 mm, cells with suberin lamellae possessed Casparian bands that had started to extend through the anticlinal walls (Fig. 4A, B). This extension did not occur in unsuberized passage cells that were usually located near the protoxylem poles. At 50 mm from the tip, U-shaped tertiary wall thickenings were first observed and were present only in suberized endodermal cells. Also at this distance, early metaxylem vessel walls and those in the pith region became lignified. The U-shaped wall thickenings continued to enlarge (Fig. 4C, D) and by 100 mm from the tip, they had reached their maximum size; few passage cells remained. These U-shaped thickenings stained positively for lignin (Fig. 4F) and autofluoresced with UV light (Fig. 4H). Although suberin was detected as a lamella in each of these cells, it was absent from the U-shaped thickenings (Fig. 4D, E, G). By this stage, the late metaxylem vessel walls had lignified. After digesting the tissue with sulfuric acid, the walls of the endodermis, mature xylem vessels and modified parenchyma

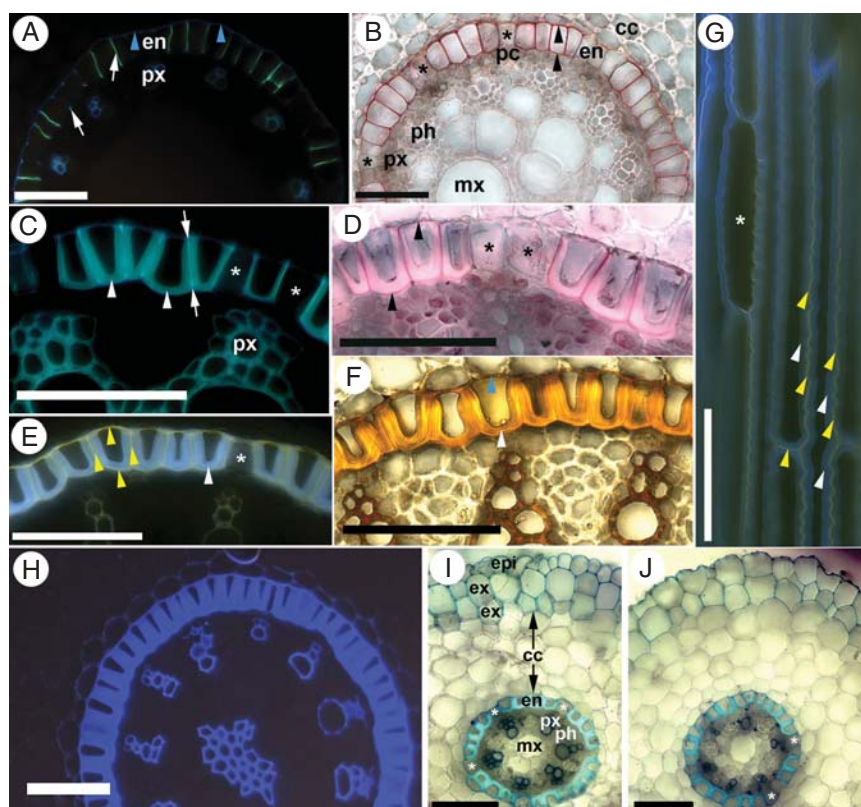


FIG. 4. Photomicrographs of (A–F, H–J) cross- and (G) longitudinal sections from *I. germanica* roots. Values in millimetres refer to distances from the root tips. (A) 30 mm. Stained with berberine hemisulfate–aniline blue. The endodermis had Casparian bands (white arrows) that either appeared dot-like or extended throughout the anticlinal walls. Autofluorescence (blue arrowheads) was observed in the outer tangential walls of the endodermal cells and in protoxylem vessel walls. (B) 30 mm. Stained with Sudan red 7B. Endodermal cells contained suberin lamellae (black arrowheads) when the Casparian band had extended through their anticlinal walls. (C) 90 mm. Stained with berberine hemisulfate–aniline blue. Mature endodermis with U-shaped wall thickenings (white arrowheads) and Casparian bands (between arrows). (D) 90 mm. Stained with Sudan red 7B. Mature endodermis with suberin lamellae (black arrowheads) that were exterior to the U-shaped wall thickenings (white arrowhead). (E) 100 mm. Stained with Fluorol yellow 088. Mature endodermis with suberin lamellae (yellow arrowheads) surrounding the wall thickenings (white arrowhead). (F) 100 mm. Stained with phloroglucinol–HCl. Lignin appeared reddish-orange in the wall thickenings (white arrowhead), the outer tangential cell walls of the endodermis (blue arrowhead) and in xylem vessel walls. (G) 100 mm. Stained with Fluorol yellow 088. Suberin lamellae (yellow arrowheads) were positioned in between wall thickenings (white arrowheads). A short passage cell (*) without suberin lamellae or wall thickenings was evident. (H) 90 mm. Unstained and viewed with UV light. Note autofluorescence of endodermal wall thickenings, and walls of xylem vessels and modified parenchyma in the pith. (I) Lateral root in cross-section, stained with TBO. Lignified walls stained blue. (J) Same as (I), but the epidermis had been sloughed off. Asterisks indicate passage cells. Abbreviations: epi, epidermis; ex, exodermis; cc, central cortex; en, endodermis; pc, pericycle; px, protoxylem; mx, metaxylem; ph, phloem. Scale bars = 100 μ m.

in the pith were retained. Dissolved structures included the U-shaped wall thickenings, pericycle, phloem and immature vessels (data not shown). Observing the inner part of the root longitudinally revealed its three-dimensional structure. Dimorphy was seen in the endodermis, where the shorter cells were without suberin lamellae and tertiary wall thickenings and, thus, were passage cells (Fig. 4G). Mature xylem vessels had reticulate wall thickenings and simple perforation plates (data not shown).

Soil-grown lateral roots. Some observations of lateral root development and anatomy were also made. Lateral root primordia initiated from the pericycle grew through the central cortex in the wake of a digestive pocket. However, they physically broke through the exodermis. The area of the exodermis thus wounded was sealed shut with a collar of modified cells that were suberized and lignified (data not shown). In general, lateral root anatomy was similar to that of the adventitious roots, except that laterals were substantially thinner, and their late metaxylem vessels were located in the centre of the root instead of a pith (Fig. 4I). The epidermis of lateral roots was not always present; it could be sloughed off (Fig. 4J).

Hydroponically grown roots. When *I. germanica* plants were grown with their roots completely submerged in nutrient solution, the onset of exodermal maturation occurred further from the root tip compared with soil-grown roots (Fig. 5). Exodermal Casparian bands and suberin lamellae were first detected in some cells of the outermost cortical cell layer of hydroponically grown roots 60 mm from the root tip compared

with 10 mm in soil-grown roots. All cells of the first exodermal layer of hydroponically grown roots had formed typical Casparian bands and suberin lamellae at 80 mm (between 5 and 6 d old) compared with 20 mm (between 1 and 2 d old) in soil-grown roots (Fig. 5; see Fig. 3A, B). In the maturing second exodermal layer of hydroponic roots, Casparian bands and suberin lamellae were found in some cells 170 mm from the root tip compared with 30 mm in soil (Fig. 5). All cells of the second exodermal layer of hydroponically grown roots matured to State II 200 mm from the tip (about 14 d old) compared with 70 mm (between 4 and 5 d old) in soil-grown roots (see Fig. 3C, D). In hydroponics, no cells of the third exodermal layer had begun to mature by 200 mm from the tip, whereas in soil some cells of this layer had begun to mature at 70 mm. Unlike the exodermis, endodermal maturation occurred as close to the tip in hydroponic roots as in soil roots.

Air gap-treated roots. The submerged part of air gap-treated roots had an exodermal anatomy like that of completely submerged roots with maturation of the first exodermal layer finishing at 80 mm from the tip (between 5 and 6 d old; Fig. 5). In air gap-treated roots, the second exodermal layer matured close to the air gap–solution interface, 100–120 mm from the tip. The second exodermal layer, with a ccCb and suberin lamellae, completed maturing by 120 mm (between 8 and 9 d old). Exodermal anatomy was nearly identical in the region of root exposed to the humid air gap (120–170 mm from the tip, between 9 and 12 d old). This 50-mm-long root zone had been exposed to humid air for 7 d (Fig. 5). The third layer had not begun to mature by 200 mm. The air gap treatment brought about a precocious maturation of the second exodermal layer, more resembling the soil-grown root than the control hydroponically grown root (Fig. 5). Since the endodermis had already reached State III of maturity 100 mm from the tip in the air gap growth condition, as well as in the other two growth conditions (Fig. 5), it was not surprising that endodermal anatomy in the part of the root exposed to the air gap was similar to roots grown in the other conditions. The average relative humidity in the air gap was 92 %.

Aeroponically grown roots. As with completely submerged, hydroponically grown roots, the exodermal maturation of aeroponically grown roots occurred further from the root tip compared with soil-grown roots (Fig. 5). In fact, the maturation sequence was similar in aeroponically and hydroponically grown roots (data combined in Fig. 5). For example, two complete exodermal layers were not observed until 200 mm from the tip (about 14 d old). This anatomy resembled that of soil-grown roots at 70 mm from tip (between 4 and 5 d old; see Fig. 3C, D). Endodermal maturation in aeroponic roots occurred at a similar distance from the tip as in roots grown in all other conditions (Fig. 5).

Ferrous sulfate toxicity in Z. mays roots

Zea mays roots that were exposed to FeSO_4 had reduced growth rates compared with the control (Fig. 6). For the 0.5 mM FeSO_4 for 2- and 3-h and 1.0 mM FeSO_4 for 2-h exposures, there were few or no measurable increases in root length. Roots exposed to 0.25 mM FeSO_4 for 2 h had growth

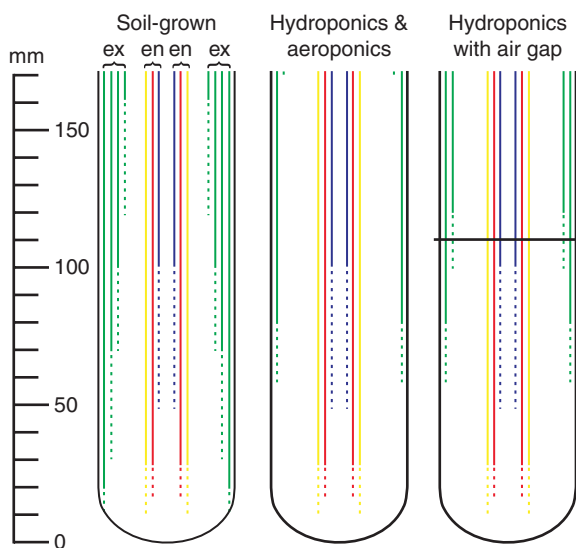


FIG. 5. Diagrams of key exodermal and endodermal developmental stages in *I. germanica* roots that were grown in different conditions. According to the growth rates, the proximal ends of the illustrated roots were 12 d old. The vertical scale refers to distance from the root tip. Green lines indicate concurrent exodermal Casparian band and suberin lamellae development; yellow lines, endodermal Casparian bands; red lines, endodermal suberin lamellae; blue lines, endodermal tertiary wall thickenings; dashed coloured lines, the structure had not yet completely developed in all cells; continuous coloured lines, the structure had completed developing in all exodermal cells or the majority of endodermal cells (i.e. few passage cells remained). The horizontal line across the air gap root marks the interface between the air gap and nutrient solution. Abbreviations: ex, exodermis; en, endodermis.

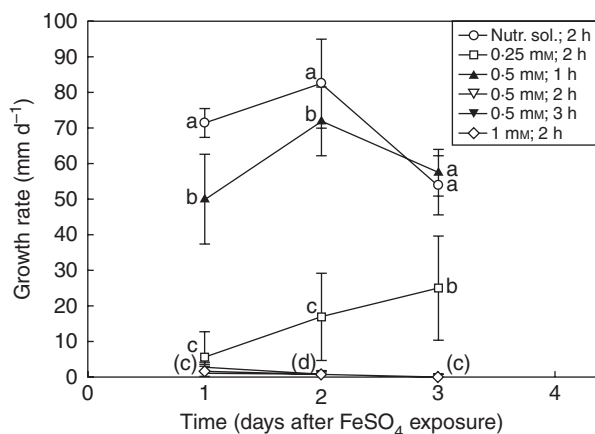


FIG. 6. The effect of FeSO_4 exposure on the growth rates of *Z. mays* roots. Values are means \pm s.d. ($n = 10$) that were pooled from two independent trials. Root growth per day refers to the time following the FeSO_4 treatment. Different letters within each day indicate significant differences (ANOVA with LSD, $P \leq 0.05$). Letters in brackets are shared by the 0.5 mM FeSO_4 for 2- and 3-h exposures and 1.0 mM FeSO_4 for 2-h exposure.

rates that were initially minimal, but increased over the next 2 d. Roots exposed to 0.5 mM FeSO_4 for 1 h had growth rates greater than roots exposed to any of the other FeSO_4 treatments, but still significantly lower than the control until day 3 (Fig. 6).

Root permeability to apoplastic tracers

Using berberine as a tracer necessitated the observation of two controls. First, unstained root sections were irradiated with UV light. Faint blue autofluorescence was observed in the walls of the exodermis, endodermis, lignified xylem vessels, and modified parenchyma in the stele (Fig. 7A, see Figs 3I and 4H). Secondly, root sections were stained directly with berberine hemisulfate. Then all cell walls of the epidermis and cortex (including those of the exodermis and endodermis) took up the fluorochrome and fluoresced yellow (Fig. 7B). When an intact root was treated externally with berberine, the dye entered the cortex and stele close to the tip where the first exodermal layer had not yet matured (< 20 mm from the tip; Fig. 7C). Beyond 20 mm, the dye penetrated and stained the walls of the epidermis and the outer tangential walls of the first layer of exodermis, but its further entry was blocked by the Casparian band in the first exodermal cell layer (Fig. 7D). When berberine was applied simultaneously to the epidermis and central cortex, it moved freely in the epidermal cell walls, walls of cortical parenchyma, walls of immature exodermal layers and the inner tangential walls of the innermost mature exodermal layer. However, the dye did not penetrate the anticlinal walls of a mature exodermis (Fig. 7E).

When FeSO_4 was used as a tracer, both unstained and stained controls were necessary. Unstained cross-sections lacked blue pigmentation (data not shown). When cross-sections were exposed to FeSO_4 and mounted in $\text{K}_4[\text{Fe}(\text{CN})_6]$ many, but not all, contained blue $\text{Fe}_4[\text{Fe}(\text{CN})_6]_3$ in every cell wall (Fig. 7F). When intact roots were exposed to FeSO_4 , variable results were obtained. In areas of the root within 20 mm from the tip,

the ferric ions entered the central cortex and stele (Fig. 7H). As the MEX matured, the outermost Casparian band did not always prevent the ions from permeating through the apoplast. For example, instances were seen where the ion penetrated through the anticlinal walls of the first and second mature exodermal layers (Fig. 7G). Ferric ions were not detected permeating deeper than two exodermal layers. Frequently, however, ferric ions were blocked at the location of the Casparian band in the first exodermal cell layer (Fig. 7I). When the root segments' peripheral layers were cut, an unexpected result was observed. In the majority of cases, ferric ions were detected penetrating the walls of only two cortical cell layers. In the few instances where the ions were observed entering deeper into the central cortex, their transport was restricted to the cell walls subjacent to the mature exodermis. The ions did not penetrate the anticlinal walls of the innermost mature exodermal layer (Fig. 7J).

To understand the reason for the variable FeSO_4 permeability results, a third apoplastic tracer experiment was performed. When root segments were exposed to water and then berberine, the fluorochrome did not penetrate the first exodermal layer (Fig. 7K). However, exposing root segments initially to FeSO_4 for 1 h followed by berberine altered the exodermis such that berberine was able to permeate through the exodermal walls and into the central cortex (Fig. 7L).

Mature root anatomy of other soil-grown iris species

Of the other species observed, *I. pumila* (Fig. 8A, B) and *I. pallida* (Fig. 8C, D) were very similar to *I. germanica*. On the other hand, the remaining five species each had a uniseriate exodermis and aerenchyma in the central cortex (Table 1). These species include *I. sibirica* (Fig. 8E, F), *I. spuria* (Fig. 8G, H), *I. versicolor* (Fig. 8I, J), *I. hexagona* (Fig. 8K, L) and *I. pseudacorus* (Fig. 8M, N).

DISCUSSION

The current detailed investigation of *I. germanica* root structure, development and apoplastic permeability extended the information contained in past reports (Kroemer, 1903; Shishkoff, 1986; Peterson and Perumalla, 1990; Zeier and Schreiber, 1998). *Iris germanica*'s MEX was classified by Kroemer (1903) as a 'Gemischte Interkutis' (mixed exodermis) which referred to the outermost exodermal layer as being dimorphic (i.e. having long and short cells) while all underlying layers had uniform cell lengths. Both Kroemer (1903) and Shishkoff (1986) observed this mixed exodermis in 14 species of various genera, all of which are members of the Asparagales (Table 2). In species with a dimorphic uniseriate exodermis, such as *Allium cepa* (von Guttenberg, 1968; Ma and Peterson, 2001), the shorter cells are typically passage cells with delayed suberin lamella deposition compared with the long cells. The lack of suberin lamellae allows passage cells to function as the least restrictive pathways for the radial transport of water and solutes across the exodermis. However, in the present study of *I. germanica*, suberin lamellae were deposited in the short cells as early as in the long cells. Thus, the short cells were not passage cells. This type of dimorphic layer may have evolved from the more

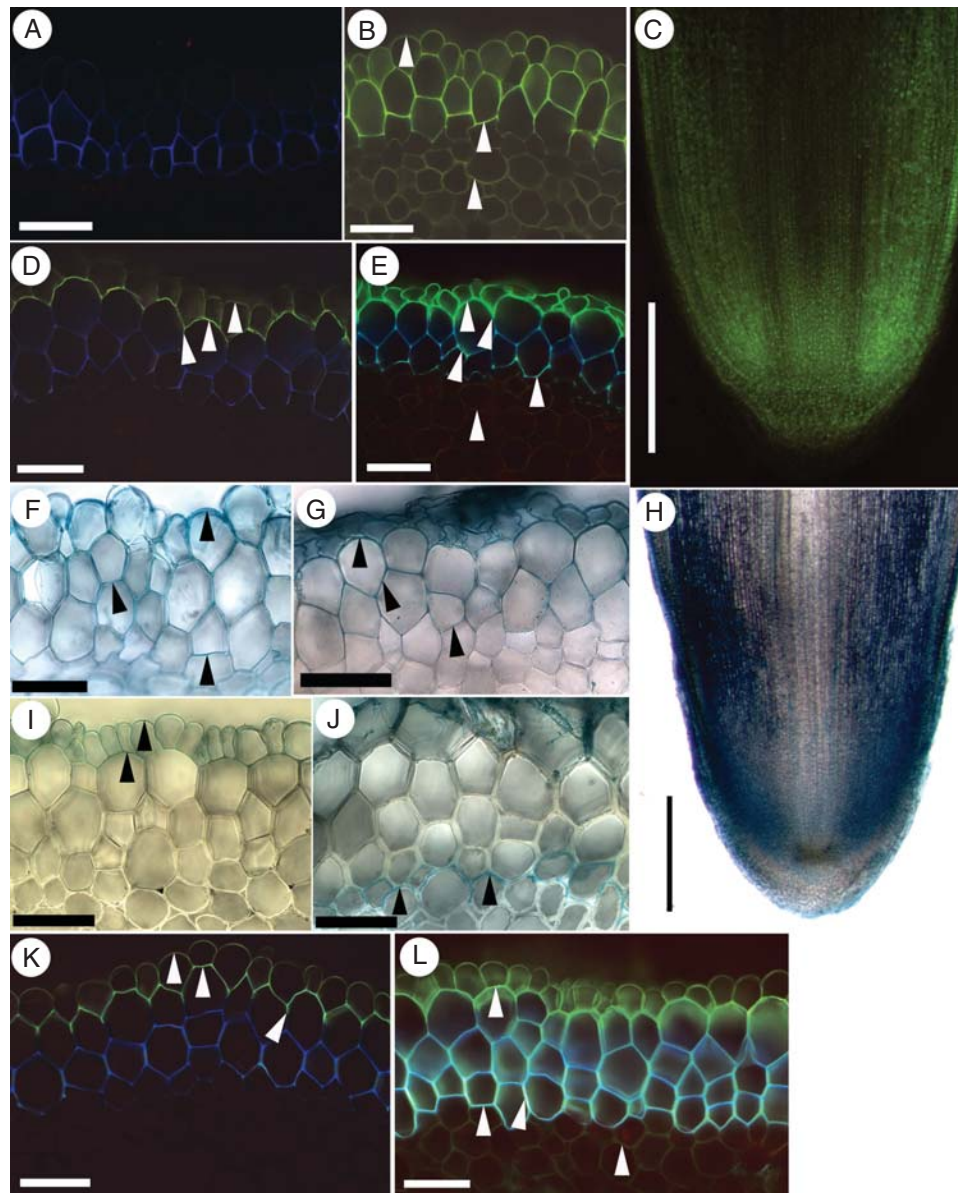


FIG. 7. Apoplastic permeability tests on *I. germanica* roots with berberine or FeSO_4 . The photomicrographs show cross-sections of the roots unless otherwise stated. Values in millimetres refer to distances from the root tips. (A) 90 mm. Unstained, UV autofluorescent control. All exodermal walls were faint blue. (B) 60 mm. Entire section stained with berberine. Epidermal, exodermal and central cortical cell walls fluoresced yellow (white arrowheads). (C) Longitudinal section of a root tip treated externally with berberine. The walls of all cells near the tip fluoresced yellow. (D) 70 mm. The outermost Casparian bands of an intact multi-seriate exodermis prevented externally applied berberine (white arrowheads) from permeating the exodermis and central cortex. (E) 70 mm. A punctured multi-seriate exodermis allowed berberine to stain the walls of epidermal, immature exodermal and central cortical cells (white arrowheads). (F) 80 mm. Entire section treated with FeSO_4 followed by $\text{K}_4[\text{Fe}(\text{CN})_6] \cdot 3\text{H}_2\text{O}$. Ferric ions precipitated in all epidermal and exodermal walls and appeared blue (black arrowheads). (G) 70 mm. Following an external treatment, ferric ions were detected in mature exodermal walls (black arrowheads). (H) Longitudinal section of a root tip treated externally with FeSO_4 followed by $\text{K}_4[\text{Fe}(\text{CN})_6] \cdot 3\text{H}_2\text{O}$. The ferric ions entered the cortex of the tip readily. (I) 90 mm. Ferric ions, as evidenced by blue precipitates (black arrowheads), were blocked from permeating the exodermal Casparian bands. (J) 90 mm. A punctured multi-seriate exodermis allowed the ferric ions limited entry to the central cortex (black arrowheads). (K) 70 mm. Intact root incubated in water and then berberine. Berberine (white arrowheads) did not permeate the Casparian bands in the first exodermal layer. (L) 100 mm. Intact root incubated in FeSO_4 and then berberine. Berberine stained the walls of all mature and immature exodermal cells, and walls of cortical parenchyma (white arrowheads). Scale bars: cross-sections = $50 \mu\text{m}$; longitudinal sections = $500 \mu\text{m}$.

common type with passage cells. *Iris germanica*'s MEX began developing from the outermost cortical layer and each subsequent layer developed centripetal to the previous one, a feature also observed by Peterson and Perumalla (1990), to a maximum of four layers.

Iris germanica's specialized exodermal Casparian band, located in the anticlinal and tangential walls as illustrated earlier by Peterson and Perumalla (1990), was termed a continuous circumferential Casparian band (ccCb; see Results above). It is proposed that ccCb be used as the standard term

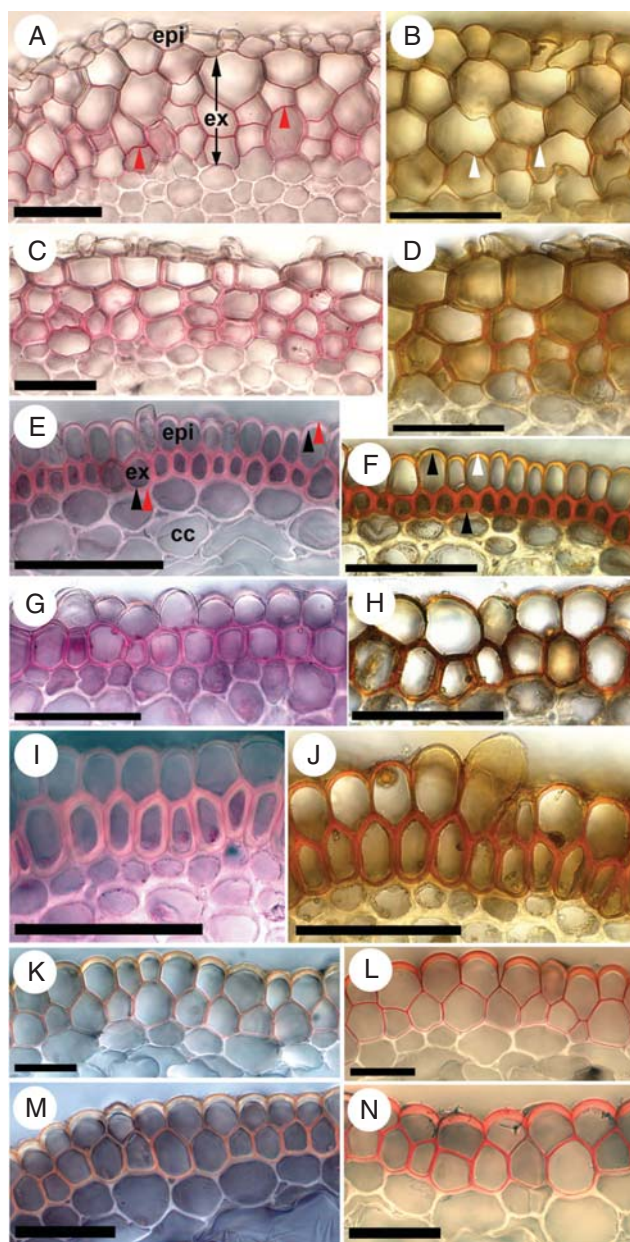


FIG. 8. Exodermis in transverse sections from soil-grown roots of various iris species. Tissue displayed in the left column was stained with Sudan Red 7B; tissue displayed in the right column was stained with phloroglucinol-HCl. Values in millimetres refer to distances from the root tips. (A, B) *Iris pumila*, 100 mm; multiseriate exodermis. (C, D) *Iris pallida*, 100 mm; multiseriate exodermis. (E, F) *Iris sibirica*, 120 mm; uniseriate exodermis. (G, H) *Iris spuria*, 90 mm; uniseriate exodermis. (I, J) *Iris versicolor*, 100 mm; uniseriate exodermis. (K, L) *Iris hexagona*, >100 mm; uniseriate exodermis. (M, N) *Iris pseudacorus*, >100 mm; uniseriate exodermis. Abbreviations: epi, epidermis; ex, exodermis; cc, central cortex. Red arrowheads indicate suberin lamellae (stained red); black arrowheads, wall thickenings; white arrowheads, lignified walls (stained reddish-orange). Scale bars = 50 μm .

when referring to this type of Casparian band, which was also detected in the roots of *Typha* spp. and *P. australis* (Seago *et al.*, 1999; Soukup *et al.*, 2002). The shape of the ccCb is dependent on that of the exodermal wall continuum (i.e. apoplast) which is governed by the orientation of MEX cells.

TABLE 1. Rhizomatous *Iris* species' natural habitats are correlated with the type of exodermis they develop and whether aerenchyma is present (+) or absent (-)

<i>Iris</i> species	Natural habitat	Type of exodermis	Aerenchyma
¹ <i>I. germanica</i> L.	Well-drained soil	Multiseriate	-
¹ <i>I. pumila</i> L.	Well-drained soil	Multiseriate	-
¹ <i>I. pallida</i> Lam.	Well-drained soil	Multiseriate	-
¹ <i>I. sambucina</i> L.*	Well-drained soil	Multiseriate	?
² <i>I. sibirica</i> L.	Water-saturated soil	Uniseriate	+
² <i>I. spuria</i> L.	Water-saturated soil	Uniseriate	+
² <i>I. versicolor</i> L.	Water-saturated soil	Uniseriate	+
² <i>I. hexagona</i> Walt.	Water-saturated soil	Uniseriate	+
² <i>I. pseudacorus</i> L.	Water-saturated soil	Uniseriate	+
² <i>I. virginica</i> L.†	Water-saturated soil	Uniseriate	+

¹, 'bearded' irises; ², 'beardless' irises.

* Observed by Kroemer (1903); † observed by Stevens (2003).

Their orientation is related to how they are generated at the root tip. For example, formation of the MEX of *Typha glauca* is initiated when the outermost layer of the ground meristem continues to divide periclinally to form multiple exodermal layers centripetally (Seago and Marsh, 1989). When *T. glauca* root is viewed in transverse section, one can observe that the periclinal divisions gave rise to an H-shaped wall continuum; hence the ccCb is also H-shaped. However, in *I. germanica* roots, the ccCb can be both H- and Y-shaped. This means that in *I. germanica*, and presumably other species with a Y-shaped ccCb, generation of the MEX at the root apical meristem differs from that of *Typha* spp. which has a tiered apex (Seago and Marsh, 1989; Heimsch and Seago, 2008). In *I. germanica*, the immature exodermal layers were not derived by a unified set of periclinal and anticlinal divisions. This was shown in transverse sections where uniform radial files were not present in the three or four cell layers across much of the immature exodermis. These ambiguous patterns of MEX development are what led to the variable ccCb shapes found in the exodermal layers. In other words, the irregular sequences of cell files derived from the open root apical meristem are reflected in the cross-sectional patterns of the later developing and mature exodermis.

Development of the endodermis in *I. germanica* was also observed progressing through States I, II and III. Casparian bands were offset toward the pericycle in cells lacking suberin lamellae, a feature also observed in *Hordeum vulgare* (barley; Robards *et al.*, 1973), *Z. mays* (Haas and Carothers, 1975) and *Triticum aestivum* (wheat, Grymaszewska and Golinowski, 1987). The presence of endodermal passage cells in mature regions far from the root tip is also common. Three striking characteristics of *I. germanica*'s endodermal cells were (1) dimorphy, (2) their palisade-like shape when viewed in cross-section and (3) their thick, lignified tertiary walls that may function in mechanical stabilization of the stele. In the dimorphic endodermis, short cells were passage cells. To the best of our knowledge, this is the first report of dimorphy in the endodermis of any species. Features (2) and (3) were also noted by Zeier and Schreiber (1998) who observed *I. germanica*'s mature (i.e. State III) endodermis with white light, fluorescence and scanning

TABLE 2. List of monocot species (class Liliopsida) that have a multiseriate exodermis and inhabit well-drained or dry substrates

Order	Family	Genus and species
Alismatales	Araceae	* <i>Philodendron wendlandii</i> Schott
Arecales	Arecaceae	* <i>Phoenix dactylifera</i> L. * <i>Phoenix roebelinii</i> O'Brien * <i>Trachycarpus fortunei</i> (Hook.) H.Wendl. * <i>Washingtonia filifera</i> (Lindl.) H.Wendl.
Asparagales	Agavaceae	* <i>Yucca recurvifolia</i> Salisb. [me] * <i>Yucca gloriosa</i> L. [me]
	Asparagaceae	* <i>Asparagus asparagoides</i> (L.) Druce * <i>Asparagus densiflorus</i> (Kunth) Jessop * <i>Asparagus officinalis</i> L. [me] * <i>Asparagus setaceus</i> (Kunth) Jessop * <i>Asparagus sprengeri</i> Regel. [me] * <i>Asparagus verticillatus</i> L. [me]
	Asphodelaceae	* <i>Asphodeline lutea</i> (L.) Reichenb. [me]
	Hemerocallidaceae	* <i>Gasteria disticha</i> (L.) Haw. * <i>Hemerocallis fulva</i> L. [me] * <i>Phormium tenax</i> Forst. & Forst. f.
	Iridaceae	* <i>Iris germanica</i> L. [me] * <i>Iris pallida</i> Lam. [me] * <i>Iris pumila</i> L. [me] * <i>Iris sambucina</i> L. [me]
	Orchidaceae	* <i>Brassavola subulifolia</i> Lindl. * <i>Cattleya aurantiaca</i> (Bateman ex Lindl.) P.N.Don
	Ruscaceae	* <i>Aspidistra elatior</i> Blume [me] * <i>Dracaena cannifolia</i> Hort. [me] * <i>Dracaena draco</i> L. [me] * <i>Sansevieria cylindrica</i> Bojer
Commelinales	Commelinaceae	* <i>Tradescantia virginiana</i> L.
Pandanales	Pandanaceae	* <i>Pandanus stenophyllus</i> Kurz
Poales	Bromeliaceae	* <i>Ananas macrodantes</i> E.Morr. * <i>Aechmea longifolia</i> (Rudge) L. B.Sm. & M.A.Spencer
	Juncaceae	* <i>Luzula sylvatica</i> (Huds.) Gaudin
	Poaceae	* <i>Chrysopogon zizanioides</i> (L.) Roberty
Zingiberales	Cannaceae	* <i>Canna indica</i> L. * <i>Canna tuerckheimii</i> Kraenzl.
	Marantaceae	* <i>Maranta arundinacea</i> L. * <i>Maranta leuconeura</i> C.J.Morren
	Strelitziaceae	* <i>Strelitzia augusta</i> Thunb.
	Zingiberaceae	* <i>Curcuma longa</i> L. * <i>Globba marantina</i> L. * <i>Hedychium coccineum</i> Buch.-Ham. ex Sm. * <i>Hedychium gardnerianum</i> Sheppard ex Ker Gawl. * <i>Zingiber officinale</i> Roscoe

Taxonomic information was referenced from the Angiosperm Phylogeny Group's website (Stevens, 2001 onwards) and Tropicos.org.

* Kroemer (1903); † Shishkoff (1986); ‡ Peterson and Perumalla (1990); [me] = mixed exodermis identified by Kroemer (1903) and Shishkoff (1986).

electron microscopy, pointing out the presence of mature wall-modifying structures.

It is well known that environmental conditions can influence plant organ growth and tissue maturation. In the current work, this was evident with regard to the timing of exodermal maturation in *I. germanica* roots that were grown in soil,

hydroponics or aeroponics. Complete exodermal development, i.e. through States I–III, occurred closer to the root tip in soil-grown roots relative to hydroponically and aeroponically grown roots. Generally, the faster a root grows in length, the further from the tip its exodermis and endodermis will develop (Wilcox, 1962; Perumalla and Peterson, 1986). Mechanical impediment of *Hordeum vulgare* non-nodal root growth was shown to induce exodermal development (Lehmann *et al.*, 2000) and limit root elongation, resulting in accelerated endodermal maturation (Wilson and Robards, 1978). However, in the present study, growth rates were remarkably similar for *I. germanica* roots grown in the various environments, indicating that factors other than growth rate were responsible for the differences in the onset of exodermal maturation. In roots grown in hydroponic and aeroponic conditions, the exodermis matured at a similar distance from the tip, and the same was true for endodermal maturation. It could be argued that these two conditions were essentially the same since the roots were always saturated with solution. Also, having a thin (10–100 µm) unstirred layer of water on the root surface, sheltered between epidermal hairs, is possible even if roots are grown in an aerated solution (Nye and Tinker, 1977; Clarkson, 1996). Miyamoto *et al.* (2001) also observed no difference in tissue development in *O. sativa* roots grown in hydroponics and aeroponics. In contrast, Zimmermann and Steudle (1998) reported that exodermal development in *Z. mays* was promoted by aeroponic conditions. In the present study, exposing hydroponically grown *I. germanica* roots to an air gap for 7 d accelerated the maturation of the second exodermal layer. Similarly, Clarkson *et al.* (1987) and Enstone and Peterson (1998) found that an air gap accelerated exodermal suberization in *Z. mays* roots within 2 d. The lower humidity levels and increased gas exchange capability within the air gap, similar to that of well-drained soil but in contrast to completely submerged conditions, may have played a role (Enstone and Peterson, 1998). The essence of all these findings is that developmental responses by plants to environmental conditions can vary depending on the species and type of condition (see Enstone *et al.*, 2003). The past and current work reveals that these responses are species-specific, making it necessary to test the reactions in each case; they cannot be assumed.

Apoplastic tracers were used to test the permeability of *I. germanica*'s exodermis. It is known that Casparian bands can limit the apoplastic flow of solutes (Enstone *et al.*, 2003) and possibly also water (Hose *et al.*, 2001). In the present study, berberine entered the root cortex and stele close to the tip where the exodermis and endodermis were immature. However, once the Casparian bands were deposited, the dye could not penetrate even a uniseriate exodermis. The current berberine tracer results are the same as those obtained with *Typha* spp. and *P. australis* (Seago *et al.*, 1999; Soukup *et al.*, 2002). Similar results were also observed by Peterson and Perumalla (1990) who used Cellufluor to test the apoplastic permeability of *I. germanica*'s mature exodermis; Cellufluor did not pass the outermost Casparian bands.

The permeability of the exodermis was also tested with ferrous sulfate. In solution, some of the ferrous ions were oxidized to ferric ions that could be precipitated in place by a subsequent application of potassium ferrocyanide (Ranathunge

et al., 2005a). This test has the advantage of using an ion of physiological interest that has a smaller molecular size than berberine. Others have used FeSO₄ as an apoplastic tracer. Soukup et al. (2002) exposed *P. australis* roots to 1 or 10–75 mM FeSO₄ for 1–24 h. Ferric ions permeated close to the tip (where the exodermis had not yet matured), but were blocked at the first mature exodermal layer (see fig. 6 in Soukup et al., 2002). Soukup et al. (2002) also observed toxicity in the form of leaky plasmalemmas when tracer exposure times exceeded 1 h. Armstrong and Armstrong (2005) exposed *Oryza sativa* roots to 2 mM FeSO₄ for 1–2 h. The corresponding images display a young (5–25 mm from the tip) exodermis (situated between the epidermis and hypodermal sclerenchyma layer) that was permeated by ferric ions. In roots grown in sulfide, permeation of ferric ions was reduced but not completely blocked by the exodermis as accumulation of the ions is noticeable in the sclerenchyma layer (see fig. 8 in Armstrong and Armstrong, 2005). Unfortunately, they did not stain for Casparian bands or suberin lamellae and it is possible that the exodermis had not matured 5–25 mm from the root tip.

In the present work, the toxicity of FeSO₄ was investigated since Soukup et al. (2002) and Ranathunge et al. (2005a) had expressed concern in using it as an apoplastic tracer. Because of the necessity of forming crystals, a minimum concentration of 0.5 mM FeSO₄ had to be used; preliminary tests showed that this was the lowest concentration that would form crystals when mixed with 1 mM K₄[Fe(CN)₆]·3H₂O (C. J. Meyer et al., unpubl. res.). In the toxicity test consisting of monitoring the growth rate of *Z. mays* roots, the time of exposure to FeSO₄ proved to be very important. Times longer than 60 min were harmful to root vitality causing significant decreases in root growth and even the complete arrest of growth at concentrations above 0.25 mM. Thus, a 1-h treatment with 0.5 mM FeSO₄ was used with *I. germanica* roots. Even with these precautions, ferric ion entry into the central cortex was restricted but not always prevented by the intact exodermis, indicating a possible toxic reaction. Toxicity became evident when root segments were pretreated with FeSO₄ followed by berberine, resulting in permeation of the latter tracer into all exodermal walls and the walls of cortical parenchyma. When introduced into the central cortex, ferric ions rarely permeated further than two cortical cell layers. This result was unexpected because the hydrated ionic radius of ferric (0.457 nm; Nightingale, 1959) should be much smaller than the diameter of the cell wall intermicrofibrillar spaces (5–30 nm; Nobel, 2005). It is possible that the concentration of ferric ions was diluted as they diffused into the free water in the cell walls, thus preventing detection by precipitation in deeper cell layers. Alternatively, attraction of the positively charged ferric ions to the walls of the first two cortical cell layers may have been strong enough to prevent deeper permeation. The problems discussed above with using FeSO₄ as an apoplastic tracer outweigh its benefits; hence, it is recommended that use of this tracer procedure be discontinued.

After observing the mature root anatomy from other rhizomatous iris species, a correlation between exodermal anatomy and habitat was noted. Those species that formed a MEX and lacked aerenchyma (*I. germanica*, *I. pumila* and *I. pallida*) live in habitats with well-drained soils. On the other hand,

species that had a uniseriate exodermis and aerenchyma (*I. sibirica*, *I. spuria*, *I. versicolor*, *I. hexagona* and *I. pseudacorus*) preferably inhabit water-saturated areas. Additionally, Stevens (2003) described the root anatomy of three wetland-living species, *I. virginica*, *I. pseudacorus* and *I. versicolor*, all of which have a uniseriate exodermis and aerenchyma. This correlation between root anatomy and habitat, however, does not extend to other taxa. From a review of the current and published data, it became clear that the majority (83 %) of species known to have a MEX are perennial monocots (eudicot exception: *Codiaeum variegatum*; Peterson and Perumalla, 1990) that inhabit well-drained substrates, and are from diverse orders within the class Liliopsida (Tables 2 and 4; Kroemer, 1903; Peterson and Perumalla, 1990). The remaining 17 % of these species are aquatic, e.g. *Typha* spp. (Seago et al., 1999), *P. australis* (Soukup et al., 2002), and an additional six species listed by Kroemer (1903), Peterson and Perumalla (1990) and Soukup et al. (2007); all of these members are of the order Poales (Tables 3 and 4). Within the Poales, the families Cyperaceae, Poaceae, Sparganiaceae and Typhaceae are positioned in three different major phylogenetic clades (see Stevens, 2001 onwards) and have variable amounts of mixed-linkage (1 → 3), (1 → 4)-β-glucans in their cell walls (see Trethewey et al., 2005). Species with a uniseriate exodermis also occupy both wet and well-drained habitats. From the known cases, 23 % of the monocots and 16 % of the eudicots inhabit water-saturated soils while the remaining majority of monocots (77 %) and eudicots (84 %) inhabit well-drained

TABLE 3. List of monocot species (class Liliopsida) that have a multiseriate exodermis and inhabit water-saturated substrates (all of these representatives are from the order Poales)

Family	Genus and species
Cyperaceae	* <i>Carex hirta</i> L.
	* <i>Schoenoplectus lacustris</i> (L.) Palla
Poaceae	# <i>Glyceria maxima</i> (Hartm.) Holmb.
	*# <i>Phragmites australis</i> (Cav.) Trin. ex Steud.
	‡ <i>Stenotaphrum secundatum</i> (Walter) Kuntze
Sparganiaceae	* <i>Sparganium emersum</i> Rehmman
Typhaceae	§ <i>Typha angustifolia</i> L.
	§ <i>Typha glauca</i> Godr.
	*† <i>Typha latifolia</i> L.

Taxonomic information referenced from the Angiosperm Phylogeny Group's website (Stevens, 2001 onwards) and Tropicos.org.

* Kroemer (1903); † Shishkoff (1986); ‡ Peterson and Perumalla (1990); § Seago et al. (1999); # Soukup et al. (2007).

TABLE 4. Number of species with a multiseriate exodermis that inhabit wet or well-drained/dry substrates*

Plant	Growth substrate		Total (%)
	No. wet (%)	No. well-drained or dry (%)	
Monocots	9 (17)	43 (83)	52 (100)

* See Tables 2 and 3 for species lists.

TABLE 5. Number of species with a uniseriate exodermis that inhabit wet or well-drained/dry substrates*

Plant	Growth substrate		Total (%)
	No. wet (%)	No. well-drained or dry (%)	
Monocots	24 (23)	80 (77)	104 (100)
Eudicots	21 (16)	108 (84)	129 (100)
Sum	45 (19)	188 (81)	233 (100)

* For species lists, see Tables S2 and S3 in Supplementary material, available online.

or dry soils (Table 5; Tables S2 and S3 in Supplementary material, available online).

It is possible that the type of exodermis confers particular advantages to aquatic plants as well as those preferring well-drained habitats. In waterlogged soils, an exodermis can restrict radial oxygen loss from the root. Radial oxygen loss occurs readily where the exodermis has not matured, such as near the root tip and in ‘windows’ where lateral roots will emerge, but is reduced in regions with a mature exodermis. Decreases in radial oxygen loss were measured across the suberized uniseriate exodermis of *O. sativa* (Armstrong and Armstrong, 2001) and *Tabernaemontana juruana* (De Simone *et al.*, 2003), and the suberized MEX of *P. australis* (Armstrong *et al.*, 2000; Armstrong and Armstrong, 2001) and *Glyceria maxima* (Soukup *et al.*, 2007). In well-drained or dry soils, the (poly)aliphatic domain of suberin lamellae in the exodermis may contribute variably to the apoplastic retention of water (Hose *et al.*, 2001). Reductions, but not blockage, in radial water permeability have been measured in roots with a mature exodermis, including *Agave deserti* (North and Nobel, 1991, 1995), *Z. mays* (Zimmermann and Steudle, 1998; Zimmermann *et al.*, 2000), *A. cepa* and *Helianthus annuus* (Taleisnik *et al.*, 1999). While a uniseriate exodermis will restrict oxygen and water from being lost to the substrate to some degree, it is presumed that multiple exodermal layers containing Casparian bands and suberin lamellae, with the correct molecular arrangements and precisely localized cell wall depositions (Bernards, 2002; Schreiber *et al.*, 2005), should provide roots with a greater resistance to oxygen loss and drought. Drought stress would occur more often to plants growing in well-drained soils than in submerged conditions. Hence, in lieu of secondary growth, perennial monocots with roots that have a MEX should be able to effectively withstand periods of drought that may be common to their natural environments. This postulate helps to explain the evolutionary specialization of the MEX.

In conclusion, a MEX, with a continuous ccCb and suberin lamellae in all cells, matured close to the root tip of soil-grown *I. germanica* roots. However, its maturation occurred much further from the tip when the roots were grown in hydroponic or aeroponic conditions. When roots were exposed to an air gap in the hydroponic chamber, maturation of the second exodermal layer was accelerated. The distance from the root tip in which the endodermis matured was not affected by the growth conditions. The root apical meristem was open and development of MEX cell files was irregular. Root growth rates were similar among the different growth conditions. Regions

of the root with an intact MEX were impenetrable to berberine but slightly permeable to ferric ions, which was likely the result of a toxic reaction. Lastly, iris species that inhabit well-drained soils have roots with a MEX while those that inhabit water-saturated substrates have a uniseriate exodermis and cortical aerenchyma. Future investigations should focus on the direct influence that a MEX may have on water and solute permeabilities and radial oxygen loss using quantitative approaches. It would also be instructive to test the mechanical strength of the lignified (and suberized) exodermis and endodermis, and to test their antimicrobial properties.

SUPPLEMENTARY DATA

Supplementary data is available online at www.aob.oxfordjournals.org/ and consists of the following tables. Table S1: List of the 25 *Iris germanica* cultivars observed for their root anatomy. All cultivars had identical root anatomy. Table S2: Monocot species with a uniseriate exodermis and various growth substrates. Table S3: Eudicot species with a uniseriate exodermis and various growth substrates.

ACKNOWLEDGEMENTS

The authors thank Prof. Dr Ernst Steudle (University of Bayreuth, Germany) for the use of hydroponic and aeroponic culture equipment, Dr Susan Mopper (University of Louisiana, Lafayette, USA) for kindly donating *I. hexagona* and *I. pseudacorus* roots, and Ms Daryl Enstone (University of Waterloo) for her invaluable technical support. This research was partially funded by a Natural Sciences and Engineering Research Council (NSERC) Discovery Grant to CAP. CJM received additional financial support from an Alexander Graham Bell Canada Graduate Scholarship (NSERC), an Ontario Graduate Scholarship (Government of Ontario, Canada) and a President’s Graduate Scholarship (University of Waterloo, Canada).

LITERATURE CITED

- Armstrong J, Armstrong W. 2001. Rice and *Phragmites*: effects of organic acids on growth, root permeability, and radial oxygen loss to the rhizosphere. *American Journal of Botany* **88**: 1359–1370.
- Armstrong J, Armstrong W. 2005. Rice: sulfide-induced barriers to root radial oxygen loss, Fe²⁺ and water uptake, and lateral root emergence. *Annals of Botany* **96**: 625–638.
- Armstrong W, Cousins D, Armstrong J, Turner DW, Beckett PM. 2000. Oxygen distribution in wetland plant roots and permeability barriers to gas-exchange with the rhizosphere: a microelectrode and modelling study with *Phragmites australis*. *Annals of Botany* **86**: 687–703.
- Bernards MA. 2002. Demystifying suberin. *Canadian Journal of Botany* **80**: 227–240.
- Bonnett HT Jr. 1968. The root endodermis: fine structure and function. *The Journal of Cell Biology* **37**: 199–205.
- Bray EA, Bailey-Serres J, Weretilnyk E. 2000. Responses to abiotic stresses. In: Buchanan BB, Gruissem W, Jones RL, eds. *Biochemistry and molecular biology of plants*. Rockville, MA: American Society of Plant Physiologists, 1158–1203.
- Brundrett MC, Enstone DE, Peterson CA. 1988. A berberine–aniline blue fluorescent staining procedure for suberin, lignin and callose in plant tissue. *Protoplasma* **146**: 133–142.
- Brundrett MC, Kendrick B, Peterson CA. 1991. Efficient lipid staining in plant material with Sudan red 7B or Fluorol yellow 088 in polyethylene glycol–glycerol. *Biotechnic and Histochemistry* **66**: 111–116.

- Clarkson DT. 1996. Root structure and sites of ion uptake. In: Waisel Y, Eshel A, Kafkafi U, eds. *Plant roots: the hidden half*, 2nd edn. New York, NY: Marcel Dekker, 483–510.
- Clarkson DT, Robards AW, Stephens JE, Stark M. 1987. Suberin lamellae in the hypodermis of maize (*Zea mays*) roots: development and factors affecting the permeability of hypodermal layers. *Plant, Cell & Environment* 10: 83–93.
- Damus M, Peterson RL, Enstone DE, Peterson CA. 1997. Modifications of cortical cell walls in roots of seedless vascular plants. *Botanica Acta* 110: 190–195.
- De Simone O, Haase K, Muller E, et al. 2003. Apoplastic barriers and oxygen transport properties of hypodermal cell walls in roots from four Amazonian tree species. *Plant Physiology* 132: 206–217.
- Enstone DE, Peterson CA. 1992. The apoplastic permeability of root apices. *Canadian Journal of Botany* 70: 1502–1512.
- Enstone DE, Peterson CA. 1997. Suberin deposition and band plasmolysis in the corn (*Zea mays* L.) root exodermis. *Canadian Journal of Botany* 75: 1188–1199.
- Enstone DE, Peterson CA. 1998. Effects of exposure to humid air on epidermal viability and suberin deposition in maize (*Zea mays* L.) roots. *Plant, Cell & Environment* 21: 837–844.
- Enstone DE, Peterson CA. 2005. Suberin lamella development in maize seedling roots grown in aerated and stagnant conditions. *Plant, Cell & Environment* 28: 444–455.
- Enstone DE, Peterson CA, Ma F. 2003. Root endodermis and exodermis: structure, function, and responses to the environment. *Journal of Plant Growth Regulation* 21: 335–351.
- Esau K. 1965. *Plant anatomy*, 2nd edn. New York, NY: John Wiley and Sons.
- Grymaszewska G, Golinowski W. 1987. The structure of the endodermis during the development of wheat (*Triticum aestivum* L.) roots. *Acta Societatis Botanicorum Poloniae* 56: 3–10.
- Guerinot ML, Yi Y. 1994. Iron: nutritious, noxious, and not readily available. *Plant Physiology* 104: 815–820.
- von Guttenberg H. 1968. Der primäre Bau der Angiospermenwurzeln. In: Linsbauer K, ed. *Handbuch der Pflanzenanatomie*, Vol. 8. Berlin: Gebrüder Borntraeger, 141–159.
- Haas DL, Carothers ZB. 1975. Some ultrastructural observations on endodermal cell development in *Zea mays* roots. *American Journal of Botany* 62: 336–348.
- Heimsch C, Seago JL Jr. 2008. Organization of the root apical meristem in angiosperms. *American Journal of Botany* 95: 1–21.
- Hose E, Clarkson DT, Steudle E, Schreiber L, Hartung W. 2001. The exodermis – a variable apoplastic barrier. *Journal of Experimental Botany* 52: 2245–2264.
- Jensen WA. 1962. *Botanical histochemistry – principles and practice*. San Francisco, CA: W.H. Freeman.
- Johansen DA. 1940. *Plant microtechnique*. New York, NY: McGraw-Hill.
- Karahara I, Shibaoka H. 1992. Isolation of Casparian strips from pea roots. *Plant and Cell Physiology* 33: 555–561.
- Kolattukudy PE. 1980. Biopolymer membranes of plants: cutin and suberin. *Science* 208: 990–1000.
- Kroemer K. 1903. Wurzelhaut, Hypodermis und Endodermis der Angiospermenwurzel. *Bibliotheca Botanica* 59: 1–148.
- Lehmann H, Stelzer R, Holzamer S, Kunz U, Gierth M. 2000. Analytical electron microscopical investigations on the apoplastic pathways of lanthanum transport in barley roots. *Planta* 211: 816–822.
- Lux A, Morita S, Abe J, Ito K. 2005. An improved method for clearing and staining free-hand sections and whole-mount samples. *Annals of Botany* 96: 989–996.
- Ma F, Peterson CA. 2001. Development of cell wall modifications in the endodermis and exodermis of *Allium cepa* roots. *Canadian Journal of Botany* 79: 621–634.
- Miyamoto N, Steudle E, Hirasawa T, Lafitte R. 2001. Hydraulic conductivity of rice roots. *Journal of Experimental Botany* 52: 1835–1846.
- Nightingale ER. 1959. Phenomenological theory of ion salvation: effective radii of hydrated ions. *Journal of Physical Chemistry* 63: 1381–1387.
- Nobel PS. 2005. *Physicochemical and environmental plant physiology*, 3rd edn. San Diego, CA: Elsevier Academic Press.
- North GB, Nobel PS. 1991. Changes in hydraulic conductivity and anatomy caused by drying and rewetting roots of *Agave deserti* (Agavaceae). *American Journal of Botany* 78: 906–915.
- North GB, Nobel PS. 1995. Hydraulic conductivity of concentric root tissues of *Agave deserti* Engelm. under wet and drying conditions. *New Phytologist* 130: 47–57.
- Nye PH, Tinker PB. 1977. *Solute movement in the soil-root system*. Oxford: Blackwell Scientific.
- O'Brien TP, Feder N, McCully ME. 1964. Polychromatic staining of plant cell walls by Toluidine Blue O. *Protoplasma* 59: 369–373.
- Pearse AG. 1968. *Histochemistry (theoretical and applied)*. London: J & A Churchill.
- Perumalla CJ, Peterson CA. 1986. Deposition of Casparian bands and suberin lamellae in the exodermis and endodermis of young corn and onion roots. *Canadian Journal of Botany* 64: 1873–1878.
- Perumalla CJ, Peterson CA, Enstone DE. 1990. A survey of angiosperm species to detect hypodermal Casparian bands. I. Roots with a uniseriate hypodermis and epidermis. *Botanical Journal of the Linnean Society* 103: 93–112.
- Peterson CA, Enstone DE. 1996. Functions of passage cells in the endodermis and exodermis of roots. *Physiologia Plantarum* 97: 592–598.
- Peterson CA, Perumalla CJ. 1990. A survey of angiosperm species to detect hypodermal Casparian bands. II. Roots with a multiseriate hypodermis or epidermis. *Botanical Journal of the Linnean Society* 103: 113–125.
- Ranathunge K, Steudle E, Lafitte R. 2003. Control of water uptake by rice (*Oryza sativa* L.): role of the outer part of the root. *Planta* 217: 193–205.
- Ranathunge K, Kotula L, Steudle E, Lafitte R. 2004. Water permeability and reflection coefficient of the outer part of young rice roots are differently affected by closure of water channels (aquaporins) or blockage of apoplastic pores. *Journal of Experimental Botany* 55: 433–448.
- Ranathunge K, Steudle E, Lafitte R. 2005a. Blockage of apoplastic bypass-flow of water in rice roots by insoluble salt precipitates analogous to a Pfeffer cell. *Plant, Cell & Environment* 28: 121–133.
- Ranathunge K, Steudle E, Lafitte R. 2005b. A new precipitation technique provides evidence for the permeability of Casparian bands to ions in young roots of corn (*Zea mays* L.) and rice (*Oryza sativa* L.). *Plant, Cell & Environment* 28: 1450–1462.
- Robards AW, Jackson SM, Clarkson DT, Sanderson J. 1973. The structure of barley roots in relation to the transport of ions into the stele. *Protoplasma* 77: 291–311.
- de Rufz de Lavison M. 1910. Du mode de pénétration de quelques sels dans la plante vivante. rôle de l'endoderme. *Revue Générale de Botanique* 22: 225–240.
- Schreiber L, Franke R, Hartmann K. 2005. Wax and suberin development of native and wound periderm of potato (*Solanum tuberosum* L.) and its relation to peridermal transpiration. *Planta* 220: 520–530.
- Seago JL Jr, Marsh LC. 1989. Adventitious root development in *Typha glauca*, with emphasis on the cortex. *American Journal of Botany* 76: 909–923.
- Seago JL Jr, Peterson CA, Enstone DE, Scholey CA. 1999. Development of the endodermis and hypodermis of *Typha glauca* Godr. and *Typha angustifolia* L. roots. *Canadian Journal of Botany* 77: 122–134.
- Shishkoff N. 1986. *The dimorphic hypodermis of plant roots: its distribution in the angiosperms, staining properties, and interaction with root-invading fungi*. PhD Thesis, Cornell University, USA.
- Soukup A, Votrubová O, Čížková H. 2002. Development of anatomical structure of roots of *Phragmites australis*. *New Phytologist* 153: 277–287.
- Soukup A, Armstrong W, Schreiber L, Franke R, Votrubová O. 2007. Apoplastic barriers to radial oxygen loss and solute penetration: a chemical and functional comparison of the exodermis of two wetland species, *Phragmites australis* and *Glyceria maxima*. *New Phytologist* 173: 264–278.
- Stevens KJ. 2003. *The role of root system characteristics in plant responses to flooding and drought*. PhD Thesis, University of Guelph, Canada.
- Stevens PF. 2001 onwards. *Angiosperm Phylogeny Website*. Version 9, June 2008 [and more-or-less continuously updated since]. <http://www.mobot.org/MOBOT/research/APweb/>
- Taleisnik E, Peyrano G, Cordoba A, Arias C. 1999. Water retention capacity in root segments differing in the degree of exodermis development. *Annals of Botany* 83: 19–27.
- Trethewey JAK, Campbell LM, Harris PJ. 2005. (1 → 3), (1 → 4)-β-D-glucans in the cell walls of the Poales (*sensu lato*): an immunogold labelling study using a monoclonal antibody. *American Journal of Botany* 92: 1660–1674.
- Tropicos.org. Missouri Botanical Garden. 27 June 2008 <<http://www.tropicos.org>>

- Van Fleet DS. 1961.** Histochemistry and function of the endodermis. *The Botanical Review* **27**: 165–221.
- Wilcox H. 1962.** Growth studies of the root of incense cedar, *Libocedrus decurrens*. I. The origin and development of primary tissues. *American Journal of Botany* **49**: 221–236.
- Wilson AJ, Robards AW. 1978.** The ultrastructural development of mechanically impeded barley roots: effects on the endodermis and pericycle. *Protoplasma* **95**: 255–265.
- Zeier J, Schreiber L. 1998.** Comparative investigation of primary and tertiary endodermal cell walls isolated from the roots of five monocotyledoneous species: chemical composition in relation to fine structure. *Planta* **206**: 349–361.
- Zeier J, Schreiber L. 1999.** Fourier transform infrared-spectroscopic characterisation of isolated endodermal cell walls from plant roots: chemical nature in relation to anatomical development. *Planta* **209**: 537–542.
- Zimmermann HM, Steudle E. 1998.** Apoplastic transport across young maize roots: effect of the exodermis. *Planta* **206**: 7–19.
- Zimmermann HM, Hartmann K, Schreiber L, Steudle E. 2000.** Chemical composition of apoplastic transport barriers in relation to radial hydraulic conductivity of corn roots (*Zea mays* L.). *Planta* **210**: 302–311.